EFFECT OF SURFACE OXYGEN GROUPS IN THE ELECTROCHEMICAL MODIFICATION OF MULTIWALL CARBON NANOTUBES BY 4-AMINO PHENYL PHOSPHONIC ACID

Andrés Felipe Quintero-Jaime[a], Diego Cazorla-Amorós[b], Emilia Morallón[a].

[a] Departamento de Química Física and Instituto Universitario de Materiales de Alicante (IUMA), University of Alicante, Ap. 99, 03080, Alicante, Spain

[b] Departamento de Química Inorgánica and Instituto Universitario de Materiales de Alicante (IUMA), University of Alicante, Ap. 99, 03080, Alicante, Spain

ABSTRACT

Electrochemical functionalization of pristine Multiwall Carbon Nanotube (MWCNT) and oxidized MWCNT with 4-aminophenyl phosphonic acid (4-APPA) has been studied. Electrochemical modification has been carried out by cyclic voltammetry using different upper potential limits, what results in the incorporation of N and P functionalities through polymerization and covalent attachment. The electrochemical characterization shows that there are important differences among the functionalized materials derived from the pristine MWCNT or the oxidized materials. For the pristine MWCNT, well-defined redox processes are observed. Characterization by X-Ray photoelectron spectroscopy, Raman spectroscopy and electron microscopy, show that oligomerization is easier for the pristine MWCNT and the presence of polymer chains are clearly distinguished for the lowest oxidation potentials. However, the presence of surface oxygen groups in the oxidized MWCNT modify the interaction of the 4-APPA with the surface promoting mainly covalent attachment.

Keywords: electrochemical modification, functionalization, phosphorus, nitrogen, MWCNT.

1. INTRODUCTION

Carbon nanotubes (CNTs) have attracted important attention over the last decades in many scientific and nanotechnology applications, due to the remarkable chemical stability, biocompatibility, catalytic and electronic properties [1]. These carbon materials can be modified through non-covalent or covalent interactions in the tip and/or the sidewall of the nanotubes [1–3]. Nowadays, tailoring the type of surface functionalities incorporated is desirable in order to develop new properties in the CNTs and improve their application in different areas like electrocatalysis and biosensing, for example [4–6].

Heteroatom doping of the carbon surface is a promising method for modifying the properties of carbon materials, which has brought remarkable improvement, for example, in the electrocatalytic behavior towards oxidation-reduction reactions, such as oxygen evolution reaction (OER) [7,8], oxygen reduction reaction (ORR) [8,9] and hydrogen evolution reaction (HER) [8,10]. Surface modification of CNT with nitrogen groups has been widely studied. The unique structure and surface properties of nitrogen-doped carbon nanotubes leads to a better dispersion of Pt that produces higher catalytic activity toward ORR [11]. Additionally, recent studies have proved the high catalytic activity for ORR of N-doped carbon materials, rising as a promising alternative in the development of catalysts for fuel cells [9]. Oxygen, nitrogen and phosphorus-doping are promising candidates to introduce functionalities, which can increase the active sites for different reactions [12,13]. Regarding P-doping of carbon materials, Berenguer et al. showed an important improvement in the stability of activated carbons towards electrochemical oxidation [14].

Carbon materials functionalization can be done through covalent and non-covalent methods [1–3]. Covalent functionalization methods employ conditions that may generate important structural changes, which can either deteriorate their structure or inhibit some of their properties. Non covalent functionalization methods are the preferred methods when it is necessary to maintain the electronic properties of the CNT.

Chemical methods are the most used for CNT functionalization. In these methods, usually the CNT are oxidized to incorporate oxygen functionalities, involving reactions of oxidation with the media, in which can be found mix of acids, O_3, UV, H_2O_2, $KMnO_4$, amount others [15,16]. Subsequently, those functionalities are either directly used or employed as intermediates to apply different organic chemistry routes, for example to introduce acyl-chloride groups and further substitution by other groups such as amines; which are useful for the grafting of other molecules, immobilization of bioreceptor elements such as DNA or in the complexation of metals for sensing applications [17–20]. Fluorination, hydrogenation, esterification, alkylation and cycle-addition, are other examples that can be found for CNT surface chemistry modification [2,21,22]. Nevertheless, chemical functionalization involves in most of the cases aggressive conditions (i.e., oxidative media), high temperature, toxic chemical reagents, etc., which in some cases produce non-controlled functionalization degree and might promote the damaging and collapse of the CNT structure [23].

On the other hand, electrochemically assisted modification of carbon materials has emerged in the last two decades as a flexible, simple and effective tool for controlled functionalization of carbon materials [2]. These methods are a promising alternative for functionalization and grafting of molecules in carbon materials, obtaining high selectivity towards the desired functional group without damage of the CNT structure [6,24].

Considering the importance to develop procedures for CNTs surface functionalization, which can provide controlled and non-damaging modification of CNT, in this study we use electrochemical methods for surface functionalization of multiwall carbon nanotubes (MWCNTs) by electrochemical oxidation in presence of 4-aminophenyl phosphonic acid (4-APPA) in aqueous solution. This will permit to incorporate both N and P heteroatoms on the MWCNT which are of great interest for different applications. In addition, we have studied the effect of the surface oxygen groups of the MWCNT on the functionalization. The results show that the degree of functionalization, electroactivity and stability of the different incorporated functionalities, is very much dependent on the surface oxygen groups present in the MWCNTs surface.

2. EXPERIMENTAL SECTION

2.1 Reagents and equipment

Multiwall Carbon Nanotubes with purity 95% (8 nm of diameter) with 10-30 μm length were purchased to Cheap Tubes Inc. (Cambridgeport, USA). Nitric acid (65%) from Panreac was employed to incorporate surface oxygen groups in the MWCNTs and also to remove the metal impurities in the CNTs. N, N-Dimethylformamide (DMF), extra pure, was provided by Scharlau and used as solvent to disperse the non-oxidized CNTs.

Sulphuric acid (98%) analytical reagent to prepare the electrolyte, was obtained by VWR Chemicals. 4-Aminophenyl phosphonic acid (4-APPA, +98%) used as modifier agent was purchased from Tokyo Chemical Industry co (TCI). Potassium dihydrogen phosphate (KH_2PO_4) was obtained from Merck. Dipotassium hydrogen phosphate tri hydrate ($K_2HPO_4 \cdot 3H_2O$) and Potassium Hydroxide (KOH, 85%) were purchased from VWR Chemicals, respectively. All the solutions were prepared using ultrapure water (18 MΩ cm, Purelab Ultra Elga equipment). The gases N_2 (99.999%) and H_2 (99.999%) were provided by Air Liquide.

2.2. Electrochemical incorporation of phosphorus and nitrogen functionalities on CNTs

2.2.1. Oxidation of pristine Multiwall Carbon Nanotubes

MWCNTs were subjected to oxidation with nitric acid solution, according to the following procedure. In a two-necked, round-bottom flask, 200 mg of MWCNTs were added in 100 mL of 3 M HNO_3 at 120ºC for 24 hours under reflux conditions. MWCNTs were separated after 24 hours, filtered, washed with ultrapure water until the pH was neutral and dried in vacuum at 60ºC for 24 hours, and weighed. The sample was named as fMWCNTs.

2.2.2. Functionalization of MWCNT and fMWCNT with 4-APPA

Working electrode was prepared using 1 mg mL^{-1} of a dispersion of each type of CNTs. DMF was used for MWCNT and water for fMWCNT, because the presence of surface oxygen groups improves the dispersibility in aqueous solution. Prior to the deposition of CNTs, glassy carbon electrode surface (3 mm diameter) was sanded with emery paper and polished using 1 and 0.05 μm alumina slurries and then rinsed with ultrapure water. Afterwards, 10 μL aliquot of the dispersion was dropped onto the glassy carbon (GC) surface and dried under an infrared lamp to remove the solvent.

Electrochemical modification was performed by cyclic voltammetry in presence of 4-APPA, using an eDAQ Potentiostat (EA163 model) coupled to a wave generator (EG&G Parc Model 175) and the data acquisition was done with an eDAQ e-corder 410 unit (Chart and Scope Software), using a standard three-electrode cell configuration. The CNTs were the working electrode (WE), a graphite rod was used as counter electrode (CE) and a reversible hydrogen

electrode (RHE) introduced in the same electrolyte without 4-APPA, was the reference electrode (RE). Electrochemical modification was carried out in 0.5 M H_2SO_4 + 1 mM 4-APPA aqueous solution in a deoxygenated cell by bubbling nitrogen. The CNTs were submitted to 10 cycles at 10 mV s^{-1} by cyclic voltammetry using different positive potential limits. After electrochemical treatment, carbon electrodes were washed with excess of water, removing the remaining electrolyte.

2.2.3. Electrochemical characterization

Electrochemical behavior of the CNTs functionalized with 4-APPA were evaluated in 0.5 M H_2SO_4 solution without 4-APPA, employing a three-electrode configuration cell. The potential range was fixed between 0 and 1 V vs. RHE at 50 mV s^{-1}.

2.3. Physicochemical characterization.

X-Ray photoelectron spectroscopy (XPS) was performed in a VG-Microtech Mutilab 3000 spectrometer and Al Kα radiation (1253.6 eV). The deconvolution of the XPS P2p and N1s peaks was done by least squares fitting using Gaussian-Lorentzian curves, while a Shirley line was used for the background determination. The P2p spectra have been analyzed considering the spin-orbit splitting into P2p3/2 and P2p1/2 with a 2:1 peak area ratio and 0.87 eV splitting [25].

Transmission electron microscopy measurements (TEM) were carried out using JEOL TEM, JEM-2010 model, INCA Energy TEM 100 model, and GATAN acquisition camera.

Temperature programmed desorption (TPD) experiments were performed in a DSC-TGA equipment (TA Instruments, SDT 2960 Simultaneous) coupled to a mass spectrometer (Thermostar, Balzers, GSD 300 T3) which was used to follow the m/z lines ascribed to the decomposition of surface functional groups from the surface of the carbon materials. The thermobalance was purged for 2 hours under a helium flow rate of 100 mL min^{-1} and then heated up to 950°C (heating rate 20°C min^{-1}).

The textural properties of the materials have been evaluated by N_2 adsorption isotherms at -196 °C in an automatic adsorption system (Autosorb-6, Quantachrome). Prior to the measurements, the samples were degassed at 250 °C for 4 h. Apparent surface areas have been determined by BET method (S_{BET}) and total micropore volumes (pores of size < 2 nm) have been assessed by applying the Dubinin-Radushkevich (DR) equation to the N_2 adsorption isotherms. Mesopore volume (V_{meso}) was determined from the difference between the volume of micropores (V_{DR}) and the volume adsorbed at a relative pressure of 0.9.

Raman spectra were collected with a Jasco NRS-5100 spectrometer. A 3.9 mW He-Ne laser at 633 nm was used. The spectra were acquired for 120 s. The detector was a Peltier cooled charge coupled device (CCD) (1024 x 255 pixels). Calibration of the spectrometer was performed with a Si slice (521 ± 2 cm^{-1}).

3. RESULTS AND DISCUSSION

3.1. Physicochemical characterization of pristine MWCNTs and fMWCNTs

MWCNT and fMWCNT were studied by temperature programmed desorption (TPD) in order to analyze the surface oxygen groups incorporated during the oxidation with HNO_3. Figure 1 shows the evolution of CO and CO_2 during the TPD for pristine MWCNTs and fMWCNTs. Table 1 reports the amount of CO and CO_2 desorbed, as well as the total oxygen

amount (calculated as CO + 2CO_2) obtained from the TPD experiments for both samples. In the case of pristine MWCNTs CO and CO_2 desorptions are very small and can be associated with the presence of some surface oxygen groups, most of them, at the end-tips of the CNTs. In the case of fMWCNT, the oxidation treatment increases the amount of surface oxygen groups, as deduced from the increase of CO and CO_2 evolution. Surface oxygen groups decompose as CO_2 between 200-400ºC, 400-550ºC and 700-900ºC associated with carboxylic acid, anhydrides and lactones, respectively [26–28]. The CO profile of fMWCNT shows main desorption peaks above 600ºC associated with phenol and carbonyl/quinone groups [26–30]. The contribution below 600ºC corresponds to anhydrides [28,30]. The results from the nitric acid treatment are in agreement with previous studies from our research group [30] and the abundant literature regarding wet oxidation of porous carbons (see for example, references [26,27,29]).

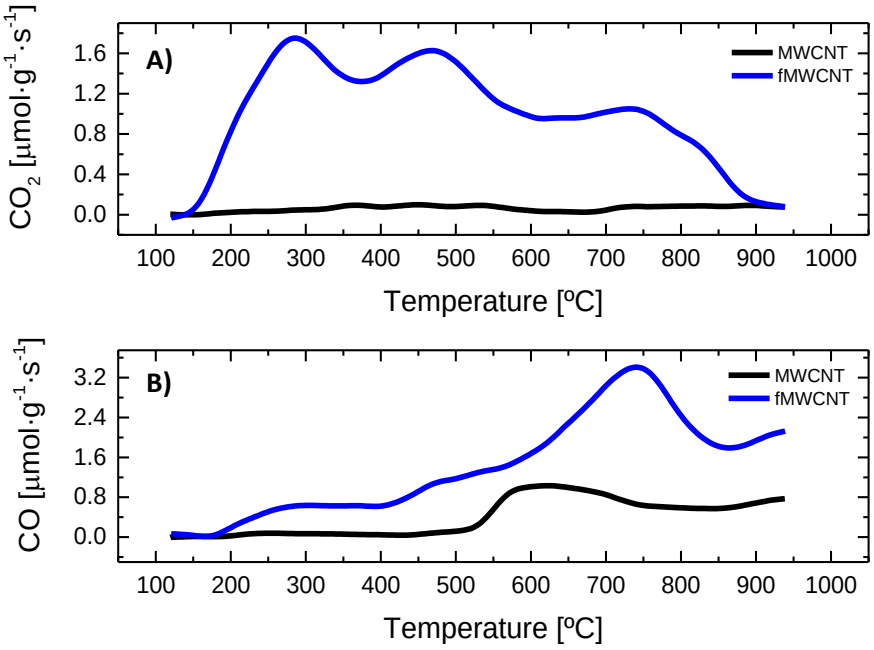

Figure 1. TPD profiles for: A) CO_2 and B) CO for pristine MWCNT and fMWCNT.

Additionally, this oxidation treatment causes an increase in the specific surface of the MWCNTs from 208 m^2 g^{-1} for pristine MWCNT to 460 m^2 g^{-1} for fMWCNT as can be observed in the N_2 isotherms in Figure 2 and Table 1.

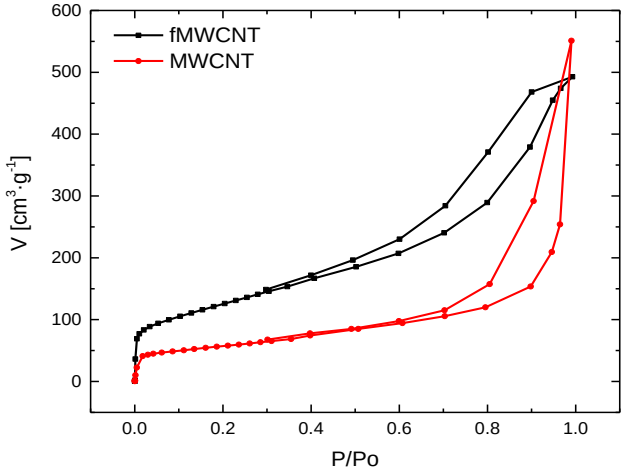

Figure 2. N_2 adsorption isotherms at -196 ºC for MWCNT and fMWCNT samples.

Table 1. Porous texture and surface chemistry characterization for both carbon nanotubes.

Sample	S_{BET} / $m^2 g^{-1}$	V_{DR} (N_2) / $cm^3 g^{-1}$	V_{meso} (N_2) / $cm^3 g^{-1}$	CO_2 / µmol g^{-1}	CO / µmol g^{-1}	Total O / µmol g^{-1}
MWCNT	208	0.08	0.29	148	954	1250
fMWCNT	460	0.18	0.57	2477	3502	8456

3.2. Electrochemical modification with 4-APPA

Optimal electrochemical functionalization conditions for MWCNT and fMWCNT with 4-Aminophenyl phosphonic acid were stablished by step-wise opening of the upper potential limit of the cyclic voltammogram from 0.8 to 1.8 V, in presence and absence of the 4-APPA (Figure 3).

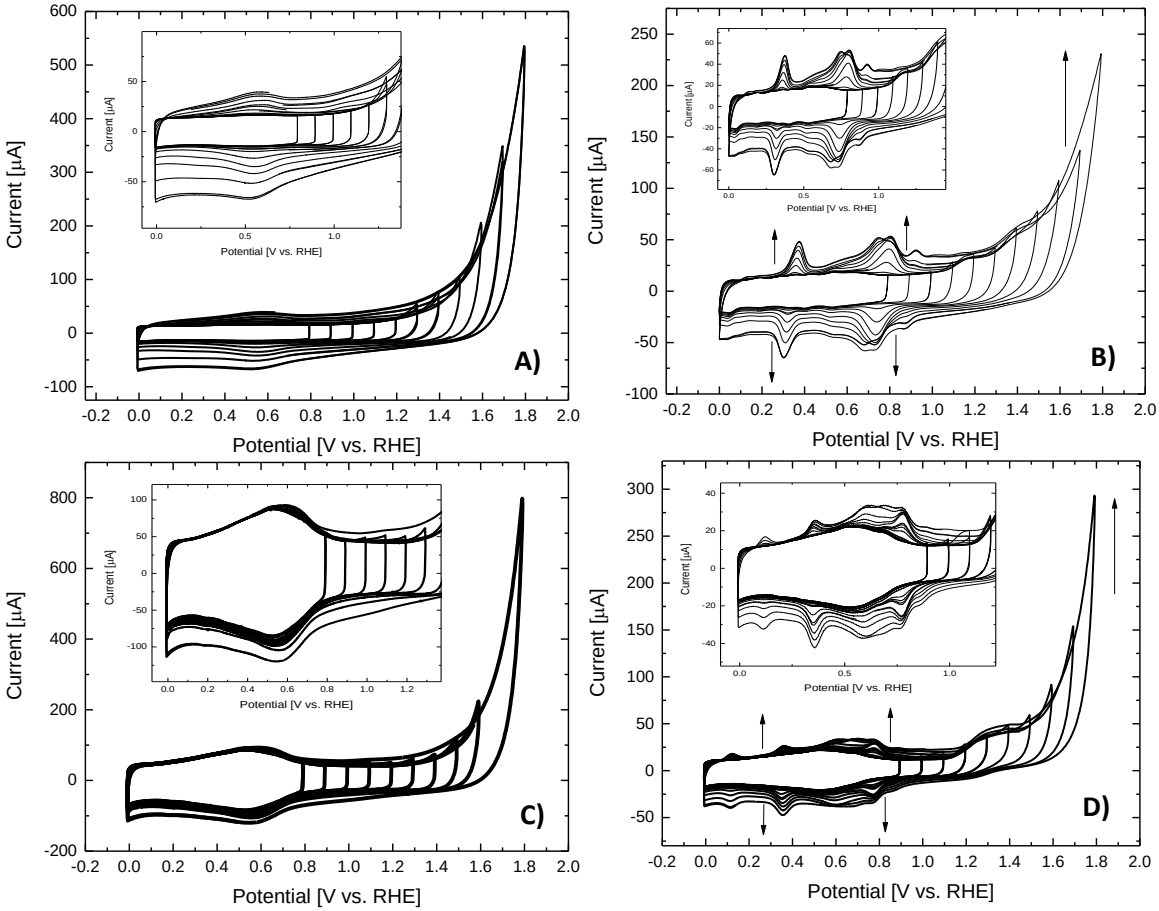

Figure 3. Cyclic voltammograms of the open step-wise positive potential limit for: A) MWCNT in 0.5 M H_2SO_4, B) MWCNT in 0.5 M H_2SO_4 + 1 mM 4-APPA, C) fMWCNT in 0.5 M H_2SO_4 and D) fMWCNT in 0.5 M H_2SO_4 + 1 mM 4-APPA.

The voltammograms for MWCNT until 1.2V present the typical rectangular-shape capacitive behavior with lack of redox processes [31,32]; however, when the upper potential limit increases over 1.4 V, oxidation/reduction processes appear at around 0.6 V, which can be associated with the surface oxygen groups produced during the oxidation of the CNTs at high potentials [33]. In contrast, fMWCNT presents from the first cycle the oxidation/reduction processes at around 0.6 V, which are related with the surface oxygen groups produced with the nitric acid treatment [30,33]. In this case, treatment with nitric acid solution induces the formation of different oxygen functionalities, among which quinone species have electrochemical activity at those potential ranges [30]. Interestingly, negligible increase in the current of these processes is observed when

the upper potential limit increases, suggesting that additional oxidation of the fMWCNT during the electrochemical treatment is not significant.

Once, 4-APPA is incorporated in the electrolyte (Figures 1-B and 1-D), no variation of the electrochemical behavior for both carbon nanotube samples occurs until 1.0 V. When the potential increases to values higher than 1 V, an over oxidation current at higher potentials occurs and different redox processes are observed in the voltammograms at around 0.75 V, 0.31 V and 0.12 V, suggesting the formation of different electrochemical species from the 4-APPA oxidation. Continuous increase in the upper potential limit generates other redox processes in the whole voltammogram, which at the same time shows an important increase in the electric charge with cycling.

From these results, the direct oxidation of both CNTs was performed with different samples in absence (black line) and presence (red line) of the 4-APPA in the electrolyte and at different positive potential limits (Figures S1 and S2). Interestingly, both CNTs show the formation of different redox processes during the oxidation of 4-APPA, and the increase in their current with cycling. It is well-known that oxidation of substituted anilines produces the polymerization of the molecule through the formation of aniline-type polymers [34,35]. Then, the oxidation of 4-APPA can promote the formation of species that can be anchored on the CNT surface or oligomers that interact with the surface of the CNTs. However, the electrochemical homopolymerization of 4-APPA on platinum electrodes is not produced, being necessary the copolymerization with aniline [36].

In this sense, Figure 4 shows the cyclic voltammograms obtained during the subsequent characterization of the different modified MWCNTs and fMWCNTs electrodes in acid media. Interestingly, well defined redox peaks observed at high potential (processes B and C) in the electrochemically modified MWCNTs do not appear in the electrochemically modified fMWCNTs, where only process A is clearly distinguished. In this last case, an increase in the charge is observed with respect to the fMWCNT treated up to the same potential limit; however, the shape of the voltammograms are similar to that of the fMWCNT. These results indicate that the presence of the surface oxygen groups in the fMWCNT affects the electrochemical oxidation of 4-APPA and the interaction with the CNT surface.

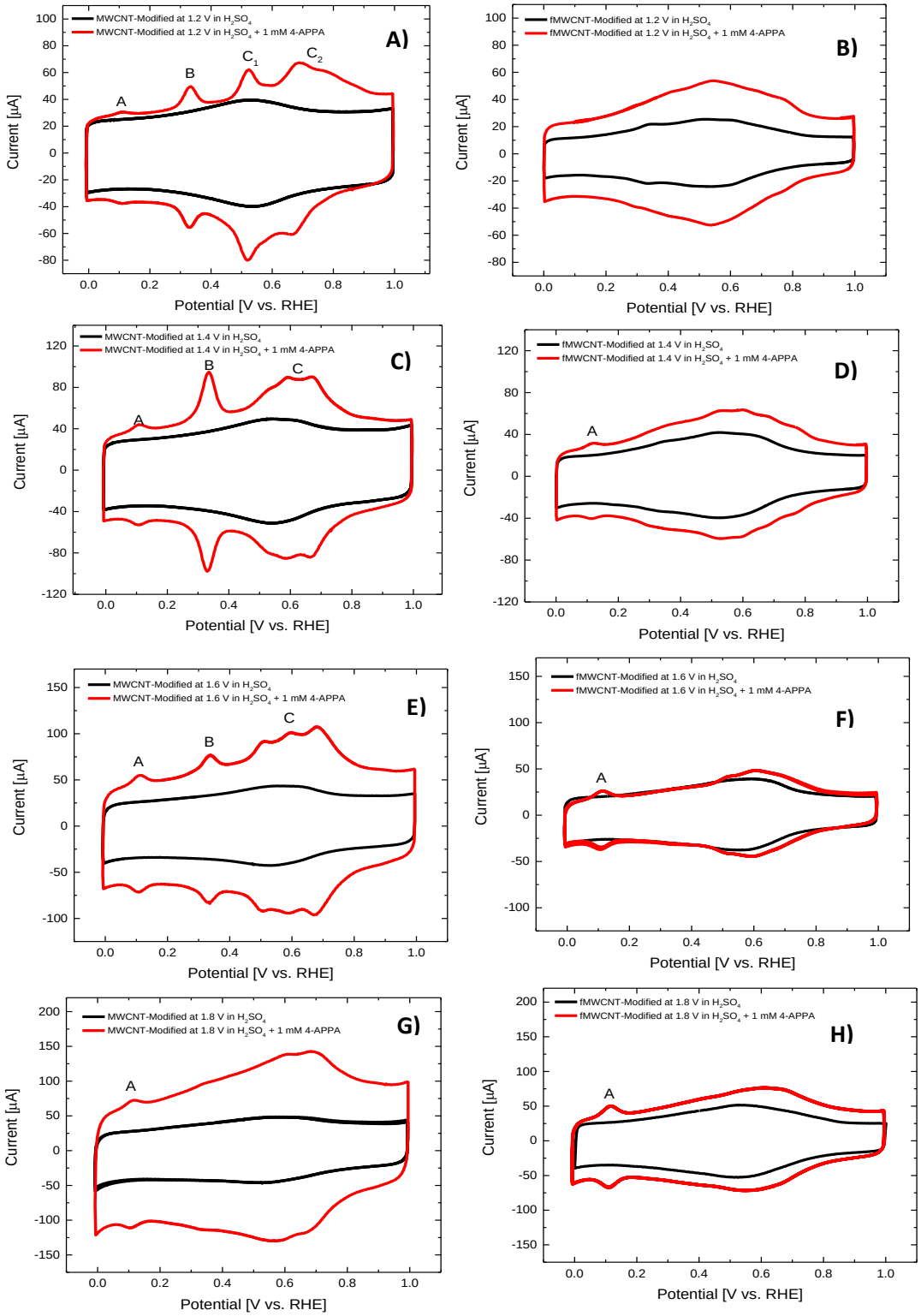

Figure 4. Cyclic voltammograms in 0.5 M H_2SO_4 at 50 mV s^{-1} of both CNTs after electrochemical modification in absence (black line) and presence (red line) of 4-APPA: A) MWCNT modified at 1.2 V, B) fMWCNT modified at 1.2 V, C) MWCNT modified at 1.4 V, D) fMWCNT modified at 1.4 V, E) MWCNT modified at 1.6 V, F) fMWCNT modified at 1.6 V, G) MWCNT modified at 1.8 V, and H) fMWCNT modified at 1.8 V.

Two different phenomena can be considered during the electrochemical oxidation in presence of 4-APPA. The first one, could be associated with a covalent attachment of the aminophenyl phosphonic acid onto the carbon nanotube through the formation of C_{CNT}-N bonds. The second phenomenon that can occur during the electrochemical functionalization, is the formation and growing of different oligomers, which can interact with the carbon nanotube walls. At the conditions used in the electrochemical oxidation, the phosphonic and the amine groups are protonated and the interaction with the surface of pristine MWCNT should mainly occur through π-π interactions between the aromatic ring of the 4-APPA molecule and the surface of the CNTs [37], what may favor polymerization reactions, thus producing electroactive species as observed in the voltammograms. In the case of the oxidized MWCNT, the presence of surface oxygen groups decreases the point of zero charge of the fMWCNT sample what would favor 4-APPA adsorption. However, the presence of electron withdrawing oxygen groups decreases the π electron density of the fMWCNT and, consequently the dispersive potential, what may result in an important decrease in 4-APPA adsorption, since the adsorption of aromatic compounds in carbon materials may be determined by dispersive forces [38]. In addition, the surface oxygen groups may also modify the orientation of the 4-APPA molecule, thus reducing the incorporation of 4-APPA parallel to the surface of the CNTs. All these factors contribute to impeding the polymerization reaction.

The current peak of the different redox processes observed in the voltammograms of the MWCNT and fMWCNT functionalized with 4-APPA (See Figures S3, S4 and S5), shows a linear-dependence with the scan rate what indicates that redox processes are surface-controlled processes [39]. At the same time, the values of the peak potential separation for all the redox processes are lower than 50 mV and the ratio of the peak currents (I_{ox}/I_{red}) is near 1 for redox processes B and C (See Table S1) suggesting a reversible behavior. Slope of the linear-fitting with the scan rate (v_{scan}) can be associated with the coverage of the active species on the surface [39]. The decrease in the slope with the potential (See Figure S5), observed in process B for MWCNT, suggests that a high oxidation potential over 1.4 V causes a decrease in the concentration of the surface species. This could be a consequence of an over oxidation of those species generated during the electrochemical functionalization onto the CNTs. Thus, in the case of the oxidation in absence of 4-APPA, the no appearance of clear redox processes in the voltammograms indicates the formation pseudocapacitive processes due to electroactive species with slightly different energy formed at the MWCNT surface, that is, electroactive oxygen functional groups. However, in presence of 4-APPA and for pristine MWCNT, a highly homogenous material seems to be formed what is in agreement with oligomerization. Some contribution from covalent 4-APPA molecules attachment on the CNT wall should not be discarded in both cases although the heterogeneity of the different sites where the reaction may occur would produce wider peaks.

3.3. Morphological characterization

Figure 5 shows the TEM images of the pristine MWCNT, the fMWCNT and after electrochemical modification with 4-APPA at different potentials.

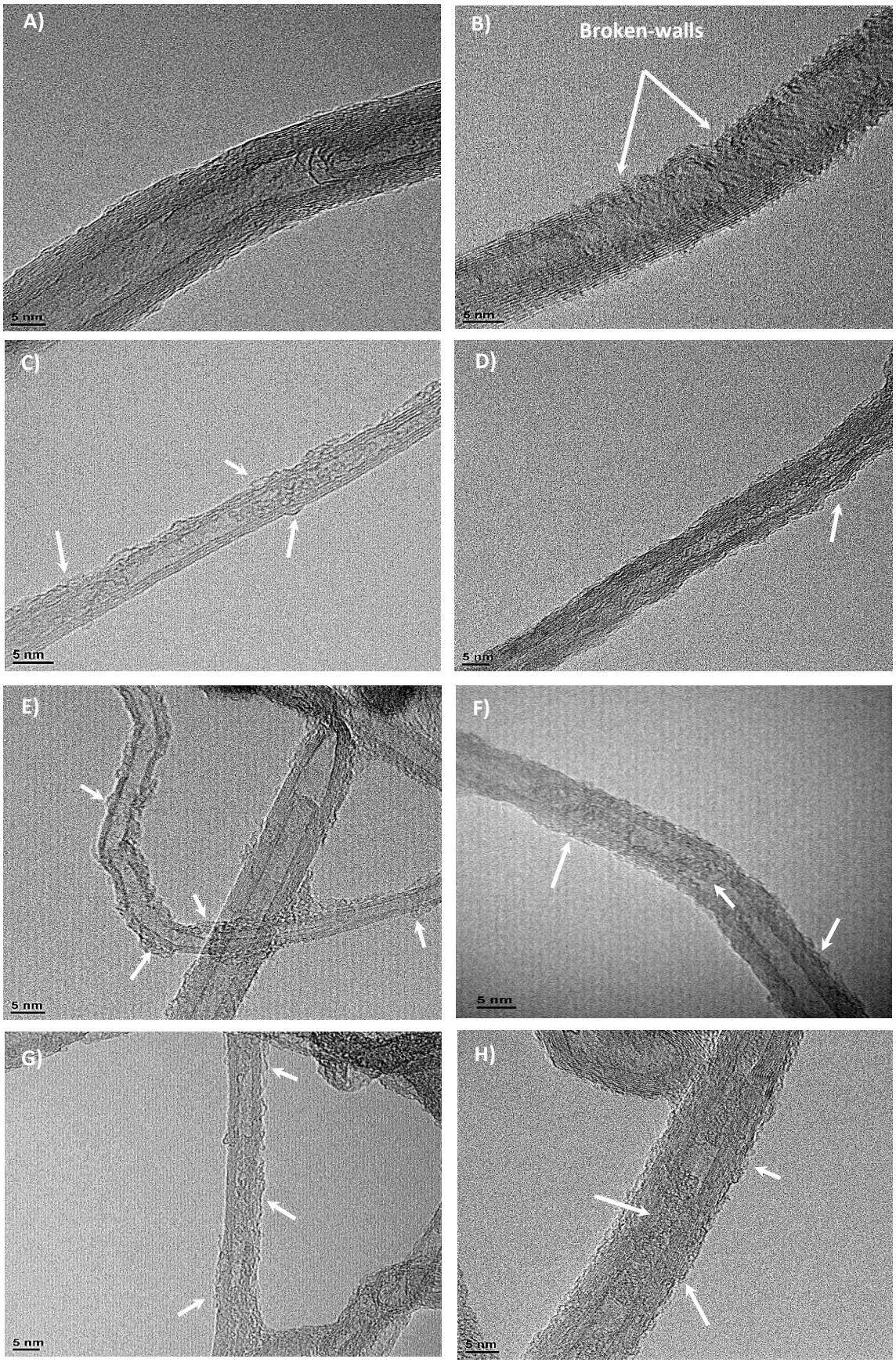

Figure 5. TEM images of: A) MWCNT, B) fMWCNT, C) MWCNT modified at 1.2 V, D) fMWCNT modified at 1.2 V, E) MWCNT modified at 1.6 V, F) fMWCNT modified at 1.6 V, G) MWCNT modified at 1.8 V and H) fMWCNT modified at 1.8 V. All the modified CNT in presence of 4-APPA.

Pristine MWCNT in Figure 5-A shows a typical tubular shape; on the other hand, fMWCNTs, which were oxidized with nitric acid, present important morphological changes with high amount of wall defects, as can be observed in figure 5-B, where broken-walls can be found. These results are in agreement with the N_2 adsorption results in which the BET surface area increases with the nitric acid treatment. Then, this treatment may permit that the inner side of the nanotubes could be accessible to the electrolyte.

Figures 5-C to H show the TEM images of the CNTs modified by electrochemical oxidation in presence of 4-APPA at different upper potential limits. The formation of agglomerates can be clearly observed onto the surface of samples MWCNT in all the positive potential limits used. These agglomerates are clearly observed in the MWCNT surface compared to fMWCNT, suggesting that oligomer chains are formed during the electrochemical modification with the 4-APPA, which can be anchored and adsorbed on the surface of the MWCNT. Interestingly, no important structural changes, as broken-walls in the graphene layers of the MWCNT sample can be observed, suggesting that despite the oxidative conditions used during the electrochemical modification most of the oxidation occurs in the 4-APPA molecules which have higher reactivity.

In the case of fMWCNT the same structures surrounding the CNT walls are also observed although in lower quantities; however, in these samples, the presence of these oligomers seem to be also observed in some cases inside the nanotubes (Figures 5-F and H), what is in agreement with the wall discontinuities observed for this material that permit the monomer and electrolyte molecules to enter into the inner part of the fMWCNT.

3.4. XPS characterization

Incorporation of different species on the CNTs surface was studied by XPS analysis. Table 2 summarizes the amount of O, N and P incorporated in the CNTs.

Table 2. Composition obtained from XPS of the electrochemical modified MWCNTs and fMWCNT with 4-APPA at different positive potentials.

Carbon nanotube	Positive potential [V vs. RHE]	O (at%)	N (at%)	P (at%)
MWCNT	Pristine	1.79	0.0	0.0
	1.2	2.53	0.49	0.25
	1.4	5.35	0.97	0.58
	1.6	7.00	1.05	0.46
	1.8	10.64	1.10	0.27
fMWCNT	Pristine	8.60	0.65	0.02
	1.2	9.30	0.89	0.15
	1.4	13.68	2.17	0.82
	1.6	10.28	1.56	0.47
	1.8	13.67	1.90	0.43

Oxygen content increases with the upper potential limit in modified MWCNT sample. This can be understood considering that, at the same time that functionalization and oligomer-chains formation take place, oxidative conditions promote the over oxidation of the polymer and of the

CNT in some extent. However, in the case of fMWCNT the oxygen content seems to reach a maximum value for oxidation potentials above 1.4V. Due to the initial strong degree of oxidation of this material, the incorporation of further oxygen species is smaller compared to the MWCNT sample which has an initial low oxygen content (Table 2). In the case of nitrogen content, it reaches a maximum value for oxidation potentials above 1.4V for both CNT samples. On the contrary, phosphorus species show a maximum value of concentration at 1.4 V, for both materials. Therefore, a desorption or decomposition process of the phosphorus groups take place at higher upper potential limits probably due to oxidation of phosphonic groups followed by hydrolysis reactions.

Figure 6 presents the XPS spectra for the CNTs modified at different positive potentials. Both CNTs show a N1s signal that can be deconvoluted into two or three contributions, which relative intensity is dependent on the functionalization potential. The three contributions observed appear at 398.5, 400 and 402.2 eV. The first and second can be assigned to imine and amine species related to the formation of oligomers similar to polyaniline structure [40,41]. The peak at 402.2 eV appears for oxidation potentials over 1.2V for the MWCNT and increases with increasing the oxidation potential. It can be associated with oxidized and positively charged nitrogen species formed from the over oxidation of the polymer at these high potentials. This tendency is also observed for the modified fMWCNT sample; however, it must be noted that this material already contains N corresponding mainly to oxidized N species due to the nitric acid oxidation pretreatment (See Table 1), what explains that this peak is also observed for the lowest oxidation potential used.

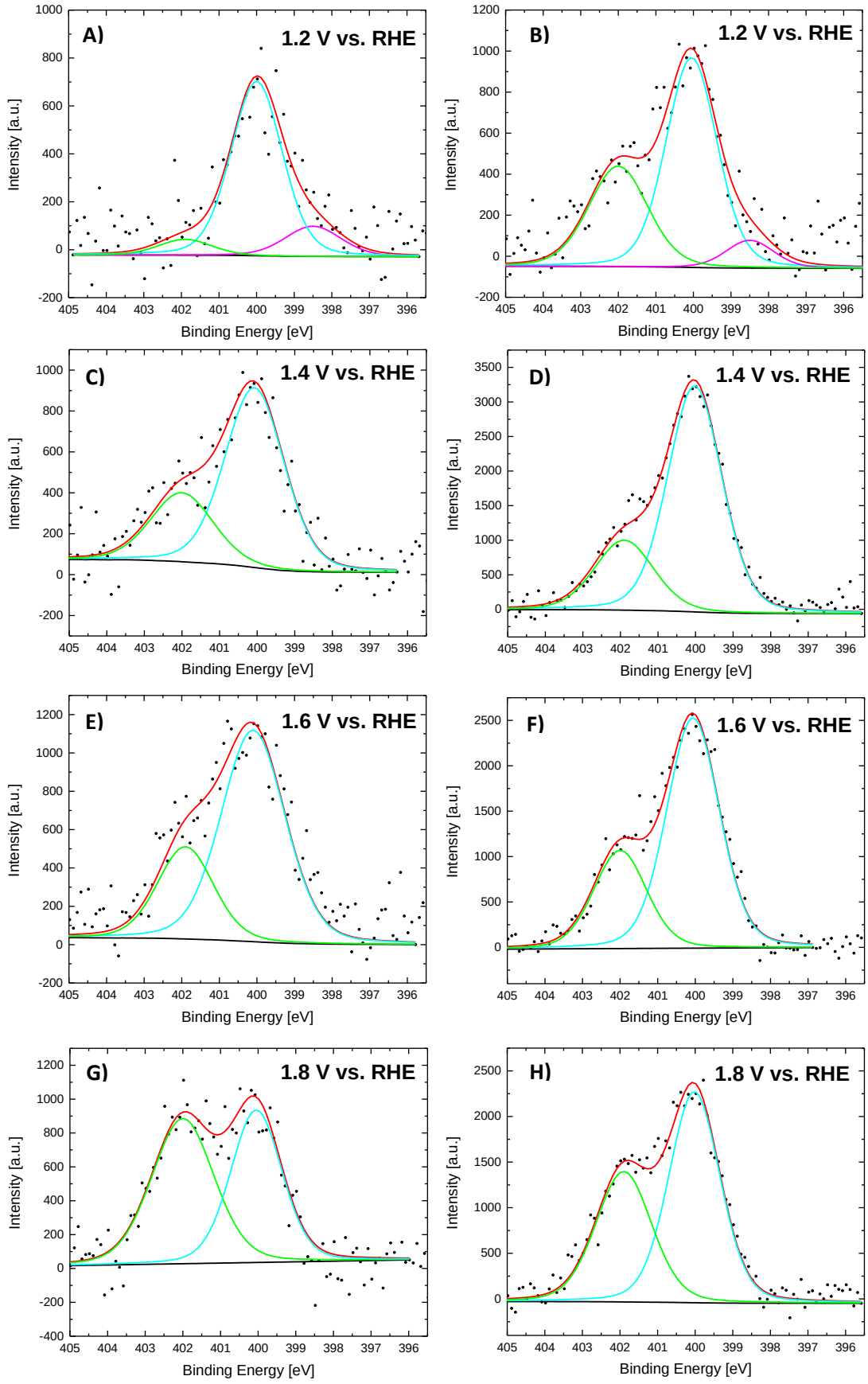

Figure 6. N1s XPS spectra for CNT electrochemically modified with 4-APPA at different applied potentials: A), C), E) and G) corresponds with MWCNT, B), D), F) and H) corresponds with fMWCNT.

Regarding the P2p spectra of the functionalized CNTs, phosphorus species present a main peak at 133.5 eV that can be deconvoluted into two contributions (Figure 7). The first doublet at 132.6 eV is associated with C-P-O species, corresponding to phosphonic group [36,42,43]. A second major contribution at 133.3 eV is clearly observed that can be associated to phosphoric species (C-O-P) [44] as consequence of the oxidation of the phosphonic group during the electrochemical oxidation conditions.

Table 3 shows the percentage of distribution for the main N and P species determined by XPS for the different functionalized CNTs. In the case of MWCNT sample, the amount of neutral N species decreases with potential with a corresponding increase in oxidized N. However, in fMWCNT the amount of neutral nitrogen species is lower since the lowest potential used and do not suffer critical oxidation, suggesting that an important amount of 4-APPA is bonded to the CNT through reactions with surface oxygen groups or surface defects. In the case of phosphorus species, most of them correspond to oxidized phosphorus species.

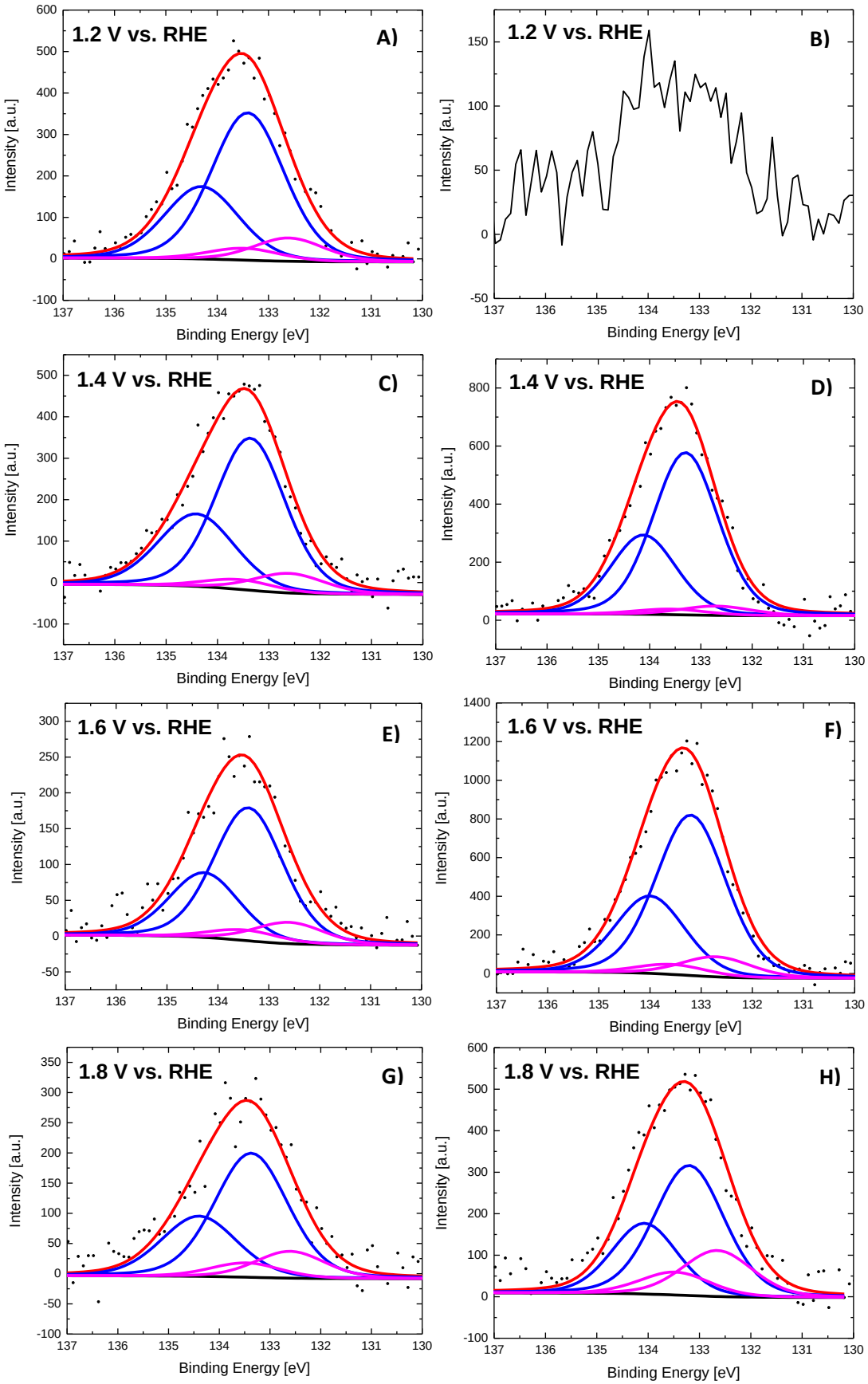

Figure 7. P2p XPS spectra for CNT electrochemically modified with 4-APPA at different upper positive limits: A), C), E) and G) corresponds with MWCNT, B), D), F) and H) corresponds with fMWCNT.

Table 3. Distribution of N1s and P2p contributions for MWCNT and fMWCNT electrochemical modified with 4-APPA at different potentials.

Carbon nanotube	Positive potential [V vs. RHE]	% Neutral N species	% Oxidized nitrogen	% C-O-P (133.3 eV)	% C-P-O (132.6 eV)
MWCNT	1.2	93	7	86	14
	1.4	71	29	89	11
	1.6	72	28	87	13
	1.8	46	54	83	17
fMWCNT	1.2	67	33	--	--
	1.4	75	25	89	11
	1.6	70	30	94	6
	1.8	60	40	74	26

*All the percentages correspond with the total amount of each N1s and P2p determined.

3.5. Raman spectroscopy

Structural and physicochemical changes were studied by Raman spectroscopy for the pristine MWCNTs and after the electrochemical modification. Figure 8 presents the Raman spectra recorded for MWCNT, fMWCNT and after electrochemical modification with 4-APPA. The first-order G and D bands (at around 1585 and 1350 cm^{-1}, respectively) are observed in all the spectra. These bands are characteristic of graphene based carbon materials, the G band corresponds to an ideal graphitic lattice vibration mode and the D band is related to the presence of defects [45–48]. More specifically, D band is related to the presence of amorphous carbon [46]. In the case of fMWCNT, the D band increases compared to MWCNT due to the nitric acid treatment that produces important damage and carbon material removal from the tube walls. In the fMWCNT sample a shoulder at around 1620 cm^{-1} is observed that can be associated to D' band (Figure 8D) due to defects along the tube induced by functionalization and strain in the C-C carbon bonds [46,47].

A low intensity band at around 1150 cm^{-1} can be clearly observed for MWCNT after modification with 4-APPA (Figure 8A). This band can be associated to C-O stretching mode in P-O-$C_{aromatic}$ species [49] or to C-N-C asymmetric stretching in quinoid structure [35, 49-51]. This feature is in agreement with oligomer formation; however, this band is not clearly distinguished for fMWCNT derived materials, what is in agreement with the lower degree of oligomer incorporation that can be achieved for the functionalized material.

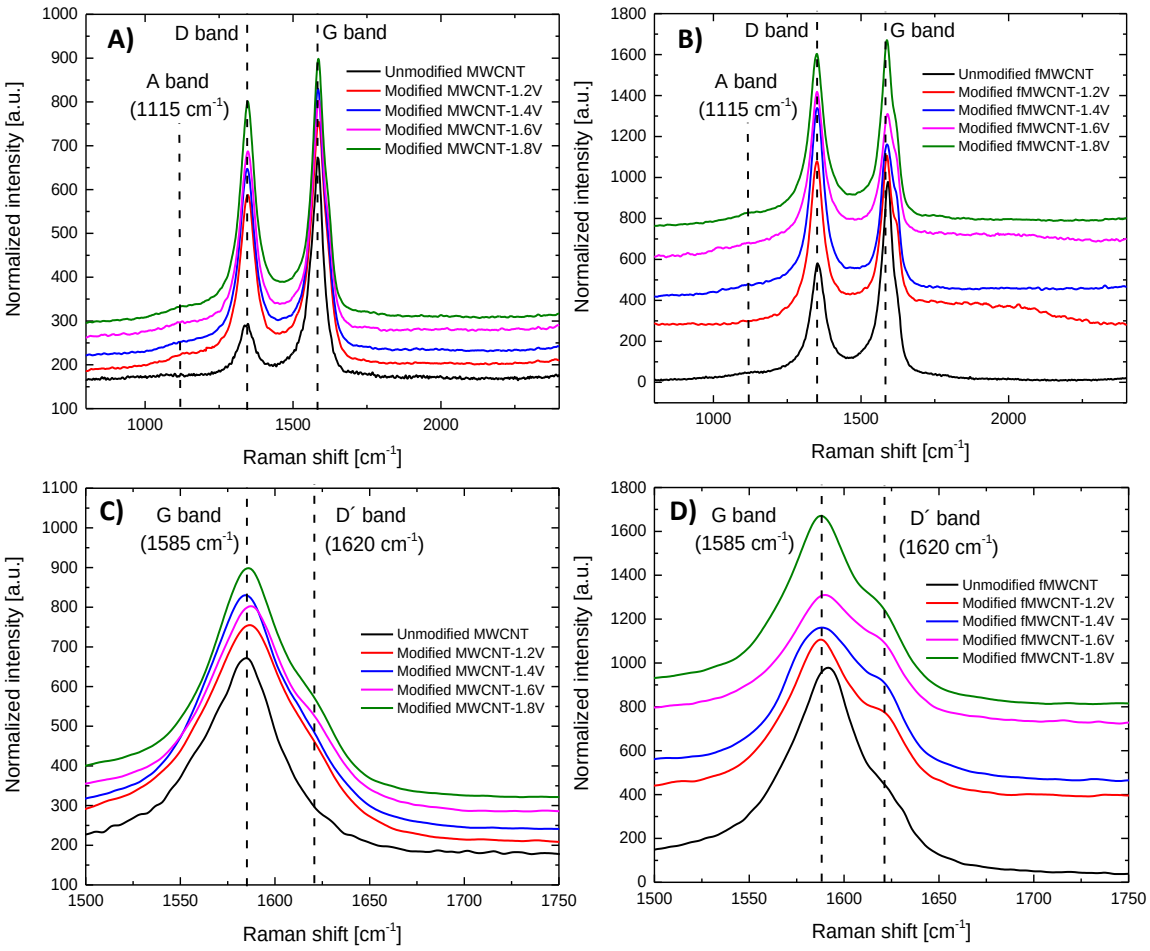

Figure 8. Raman spectra of carbon nanotubes electrochemically modified with 4-APPA at different positive potentials: A) MWCNT, B) fMWCNT, C) enlargement of G and D` region for MWCNT and D) enlargement of G and D` region for fMWCNT.

Once MWCNT and fMWCNT are submitted to a high anodic polarization in presence of 4-APPA, the D and D' bands increase. In the case of MWCNT a shoulder at around 1620 cm^{-1} can be distinguished and the D' band increases importantly for fMWCNT. The anodic polarization is inducing the formation of defects which is more important for fMWCNT. Those defects, which are present in a higher concentration for fMWCNT, can be anchoring points for 4-APPA thus unfavouring the polymerization process.

Figure 9 presents the I^D/I^G and $I^{D`}/I^G$ ratios calculated after deconvolution of the G band (See Figures S6 and S7). For curve fitting, Lorentzian shape has been used for G band and Gaussian shape for D' band [52]. The evolution of $I^D/I^G$ and $I^{D`}/I^G$ ratios with potential follows a similar trend; in the case of MWCNT materials they increase with potential and for fMWCNT it goes through a maximum. In addition, the I^D/I^G and $I^{D`}/I^G$ ratios are higher for fMWCNT derived materials for all the potentials studied except for the sample prepared at 1.8V. The increase in the ratio of bands for functionalized MWCNTs indicates some oxidation of the pristine MWCNT generating defects. It must be noted that there is an important increase after modifying the material at 1.2 V compared to the pristine MWCNT and, afterwards, the increase is not important until 1.6V. However, the increase of the ratio from the pristine fMWCNT and after modification at 1.2V is not so high because the functionalization with HNO_3 already produces important amount of defects in the MWCNT. Upon modification of fMWCNT with increasing potential the ratios

I^D/I^G and $I^{D`}/I^G$ goes through a maximum indicating that at such potential some removal of the most reactive carbon sites and amorphous carbon may occur through carbon gasification reactions or the formation of species in solution. This is in agreement with previous observations with nanostructured carbon materials [48].

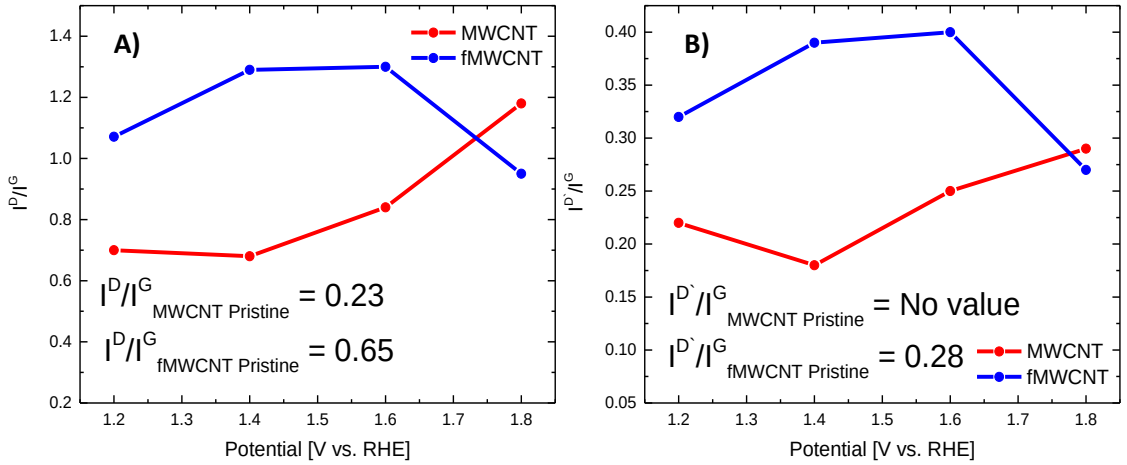

Figure 9. A) I^D/I^G ratio and B) $I^{D`}/I^G$, both as a function of the positive potential limit used in the electrochemical modification with 4-APPA.

4. Conclusions

MWCNT and fMWCNT were successfully functionalized with N and P species during electrochemical oxidation of 4-APPA employing cyclic voltammetry. The oxidation of 4-APPA promotes the formation of electroactive oligomers onto the CNT surface; however, covalently bonded redox species cannot be discarded. It has been observed a negative effect of the surface oxygen groups in the CNTs in the degree of functionalization. Thus, for the fMWCNT the amount of phosphorus incorporated is lower than in the non-oxidized MWCNT. However, the amount of P incorporated shows a maximum in both CNTs at an upper potential limit of 1.4 V; further potential increase causes an overoxidation of the oligomers or the oxidation of the phosphorus groups without producing severe damage of the carbon nanotube structure.

In the case of MWCNTs, different redox processes with high reversibility are observed, which produces a remarkable increase in the electric charge stored compared to the pristine MWCNT. In addition, oligomer chains are clearly observed by TEM. In the case of the fMWCNT, the oligomerization reaction is not favored compared to pristine MWCNT. In this material, the presence of electron withdrawing oxygen groups that decrease the π electron density of the CNT and modify the orientation of the 4-APPA molecule, thus reducing the incorporation of 4-APPA parallel to the surface of the CNTs, impede the polymerization reaction.

The evolution of I^D/I^G and $I^{D`}/I^G$ Raman band ratios with potential in presence of 4-APPA follows a similar trend for functionalized MWCNT and functionalized fMWCNT. For MWCNT they increase importantly from 1.4 V, indicating that some oxidation of the MWCNT occurs from this potential, generating defects. However, in the case of fMWCNT these ratios go through a maximum indicating that some loss of carbon material occurs through carbon gasification reactions or the formation of species in solution. These reactions may also make difficult the functionalization by 4-APPA.

Thus, the presence of surface oxygen groups in the MWCNT are detrimental to achieve the functionalization through polymerization reactions, being covalent attachment the prevailing mechanism.

Acknowledgements

The authors would like to thank MINECO and FEDER (MAT2016-76595-R) for the financial support. A.F.Q.J. gratefully acknowledges Generalitat Valenciana for the financial support through Santiago Grisolia grant (GRISOLIA/2016/084).

References

[1] A. Hirsch, Functionalization of Single-Walled Carbon Nanotubes, Angew. Chemie Int. Ed. 41 (2002) 1853–1859.

[2] C. González-Gaitán; R. Ruíz-Rosas; E. Morallón; D. Cazorla-Amorós. Electrochemical Methods to Functionalize Carbon Materials. In: T. Vijay Kumar; T. Manju Kumari, editor. *Chemical Functionalization of Carbon Materials-Chemistry and Applications*, Taylor and Francis group, CRC Press, Washington, 2016, p.p. 230-249.

[3] S. Mallakpour, S. Soltanian, Surface functionalization of carbon nanotubes: fabrication and applications, RSC Adv. 6 (2016) 109916–109935.

[4] L. Hu, D.S. Hecht, G. Grüner, Carbon Nanotube Thin Films: Fabrication, Properties, and Applications, Chem. Rev. 110 (2010) 5790–5844.

[5] V. Georgakilas, A. Bourlinos, D. Gournis, T. Tsoufis, C. Trapalis, A. Mateo-Alonso, M. Prato, Multipurpose Organically Modified Carbon Nanotubes: From Functionalization to Nanotube Composites, J. Am. Chem. Soc. 130 (2008) 8733–8740.

[6] C. González-Gaitán, R. Ruiz-Rosas, E. Morallón, D. Cazorla-Amorós, Functionalization of carbon nanotubes using aminobenzene acids and electrochemical methods. Electroactivity for the oxygen reduction reaction, Int. J. Hydrogen Energy. 40 (2015) 11242–11253.

[7] J.-C. Li, P.-X. Hou, S.-Y. Zhao, C. Liu, D.-M. Tang, M. Cheng, F. Zhang, H.-M. Cheng, A 3D bi-functional porous N-doped carbon microtube sponge electrocatalyst for oxygen reduction and oxygen evolution reactions, Energy Environ. Sci. 9 (2016) 3079–3084.

[8] C. Tang, M.-M. Titirici, Q. Zhang, A review of nanocarbons in energy electrocatalysis: Multifunctional substrates and highly active sites, J. Energy Chem. 26 (2017) 1077–1093.

[9] J. Quílez-Bermejo, E. Morallón, D. Cazorla-Amorós, Oxygen-reduction catalysis of N-doped carbons prepared via heat treatment of polyaniline at over 1100 °C, Chem. Commun. 54 (2018) 4441–4444.

[10] K. Qu, Y. Zheng, X. Zhang, K. Davey, S. Dai, S.Z. Qiao, Promotion of Electrocatalytic Hydrogen Evolution Reaction on Nitrogen-Doped Carbon Nanosheets with Secondary Heteroatoms, ACS Nano. 11 (2017) 7293–7300.

[11] Y. Chen, J. Wang, H. Liu, M.N. Banis, R. Li, X. Sun, T.-K. Sham, S. Ye, S. Knights, Nitrogen Doping Effects on Carbon Nanotubes and the Origin of the Enhanced Electrocatalytic Activity of Supported Pt for Proton-Exchange Membrane Fuel Cells, J. Phys. Chem. C. 115 (2011) 3769–3776.

[12] S. Sajjadi, H. Ghourchian, P. Rahimi, Different behaviors of single and multi wall carbon nanotubes for studying electrochemistry and electrocatalysis of choline oxidase, Electrochim. Acta. 56 (2011) 9542–9548.

[13] E. Cruz-Silva, D.A. Cullen, L. Gu, J.M. Romo-Herrera, E. Muñoz-Sandoval, F. López-

Urías, B.G. Sumpter, V. Meunier, J.-C. Charlier, D.J. Smith, H. Terrones, M. Terrones, Heterodoped Nanotubes: Theory, Synthesis, and Characterization of Phosphorus−Nitrogen Doped Multiwalled Carbon Nanotubes, ACS Nano. 2 (2008) 441–448.

[14] R. Berenguer, R. Ruiz-Rosas, A. Gallardo, D. Cazorla-Amorós, E. Morallón, H. Nishihara, T. Kyotani, J. Rodríguez-Mirasol, T. Cordero, Enhanced electro-oxidation resistance of carbon electrodes induced by phosphorus surface groups, Carbon. 95 (2015) 681–689.

[15] K.A. Wepasnick, B.A. Smith, K.E. Schrote, H.K. Wilson, S.R. Diegelmann, D.H. Fairbrother, Surface and structural characterization of multi-walled carbon nanotubes following different oxidative treatments, Carbon. 49 (2011) 24–36.

[16] V.J. González, S.M. Vega-Díaz, A. Morelos-Gómez, K. Fujisawa, M. Endo, O.M. Cadiz, J.B. Llido, M. Terrones, H2O2/UV layer-by-layer oxidation of multiwall carbon nanotubes: The "onion effect" and the control of the degree of surface crystallinity and diameter, Carbon. 139 (2018) 1027–1034.

[17] T. Ramanathan, F.T. Fisher, R.S. Ruoff, L.C. Brinson, Amino-Functionalized Carbon Nanotubes for Binding to Polymers and Biological Systems, Chem. Mater. 17 (2005) 1290–1295.

[18] E. Lafuente, M.A. Callejas, R. Sainz, A.M. Benito, W.K. Maser, M.L. Sanjuán, D. Saurel, J.M. de Teresa, M.T. Martínez, The influence of single-walled carbon nanotube functionalization on the electronic properties of their polyaniline composites, Carbon. 46 (2008) 1909–1917.

[19] P. Cañete-Rosales, M. González, A. Ansón, M.T. Martínez, C. Yáñez, S. Bollo, Electrochemical characterization of oligonucleotide-carbon nanotube functionalized using different strategies, Electrochim. Acta. 140 (2014) 489–496.

[20] M.L. Ramírez, C.S. Tettamanti, F.A. Gutierrez, J.M. Gonzalez-Domínguez, A. Ansón-Casaos, J. Hernández-Ferrer, M.T. Martínez, G.A. Rivas, M.C. Rodríguez, Cysteine functionalized bio-nanomaterial for the affinity sensing of Pb(II) as an indicator of environmental damage, Microchem. J. 141 (2018) 271–278.

[21] P.-C. Ma, N.A. Siddiqui, G. Marom, J.-K. Kim, Dispersion and functionalization of carbon nanotubes for polymer-based nanocomposites: A review, Compos. Part A Appl. Sci. Manuf. 41 (2010) 1345–1367.

[22] M. Holzinger, J. Abraham, P. Whelan, R. Graupner, L. Ley, F. Hennrich, M. Kappes, A. Hirsch, Functionalization of Single-Walled Carbon Nanotubes with (R-)Oxycarbonyl Nitrenes, J. Am. Chem. Soc. 125 (2003) 8566–8580.

[23] G. Tuci, C. Vinattieri, L. Luconi, M. Ceppatelli, S. Cicchi, A. Brandi, J. Filippi, M. Melucci, G. Giambastiani, "Click" on Tubes: a Versatile Approach towards Multimodal Functionalization of SWCNTs, Chem. – A Eur. J. 18 (2012) 8454–8463.

[24] D. Bélanger, J. Pinson, Electrografting: a powerful method for surface modification, Chem. Soc. Rev. 40 (2011) 3995–4048.

[25] T. Cordero-Lanzac, F.J. García-Mateos, J.M. Rosas, J. Rodríguez-Mirasol, T. Cordero, Flexible binderless capacitors based on P- and N-containing fibrous activated carbons from denim cloth waste, Carbon. 139 (2018) 599–608.

[26] H.P. Boehm, Surface oxides on carbon and their analysis: a critical assessment, Carbon. 40 (2002) 145–149.

[27] J.L. Figueiredo, M.F.R. Pereira, M.M.A. Freitas, J.J.M. Órfão, Modification of the surface chemistry of activated carbons, Carbon. 37 (1999) 1379–1389.

[28] M.C. Román-Martínez, D. Cazorla-Amorós, A. Linares-Solano, C.S.-M. de Lecea, Tpd and TPR characterization of carbonaceous supports and Pt/C catalysts, Carbon N. Y. 31 (1993) 895–902.

[29] C. Moreno-Castilla, M. V López-Ramón, F. Carrasco-Marín, Changes in surface chemistry of activated carbons by wet oxidation, Carbon. 38 (2000) 1995–2001.

[30] M.J. Bleda-Martínez, D. Lozano-Castelló, E. Morallón, D. Cazorla-Amorós, A. Linares-Solano, Chemical and electrochemical characterization of porous carbon materials, Carbon. 44 (2006) 2642–2651.

[31] D. Salinas-Torres, F. Huerta, F. Montilla, E. Morallón, Study on electroactive and electrocatalytic surfaces of single walled carbon nanotube-modified electrodes, Electrochim. Acta. 56 (2011) 2464–2470.

[32] C. González-Gaitán, R. Ruiz-Rosas, E. Morallón, D. Cazorla-Amorós, Effects of the surface chemistry and structure of carbon nanotubes on the coating of glucose oxidase and electrochemical biosensors performance, RSC Adv. 7 (2017) 26867–26878.

[33] F. Zaragoza-Martín, D. Sopeña-Escario, E. Morallón, C.S.M. de Lecea, Pt/carbon nanofibers electrocatalysts for fuel cells. Effect of the support oxidizing treatment, J. Power Sources. 171 (2007) 302–309.

[34] T. Lindfors, A. Ivaska, pH sensitivity of polyaniline and its substituted derivatives, J. Electroanal. Chem. 531 (2002) 43–52.

[35] A. Benyoucef, F. Huerta, J.L. Vázquez, E. Morallon, Synthesis and in situ FTIRS characterization of conducting polymers obtained from aminobenzoic acid isomers at platinum electrodes, Eur. Polym. J. 41 (2005) 843–852.

[36] Martínez-Sánchez, B. *Síntesis y Caracterización Electroquímica de Polianilinas Modificadas con Grupos Fosfónicos*, Universidad de Alicante, Master thesis, 2019.

[37] L.R. Radovic, I.F. Silva, J.I. Ume, J.A. Menéndez, C.A.L.Y. Leon, A.W. Scaroni, An experimental and theoretical study of the adsorption of aromatics possessing electron-withdrawing and electron-donating functional groups by chemically modified activated carbons, Carbon, 35 (1997) 1339–1348.

[38] J. Rivera-Utrilla, M. Sánchez-Polo, The role of dispersive and electrostatic interactions in the aqueous phase adsorption of naphthalenesulphonic acids on ozone-treated activated carbons, Carbon. 40 (2002) 2685–2691.

[39] A. Bard, L. Faulkner, Electrochemical Methods: Fundamental and Applications, 2nd ed., John Wiley & Sons, Ltd, Austin, 2000.

[40] H.S.O. Chan, S.C. Ng, W.S. Sim, K.L. Tan, B.T.G. Tan, Preparation and characterization of electrically conducting copolymers of aniline and anthranilic acid: evidence for self-doping by x-ray photoelectron spectroscopy, Macromolecules. 25 (1992) 6029–6034.

[41] J. Quílez-Bermejo, A. Ghisolfi, D. Grau-Marín, E. San-Fabián, E. Morallón, D. Cazorla-Amorós, Post-synthetic efficient functionalization of polyaniline with phosphorus-containing groups. Effect of phosphorus on electrochemical properties, Eur. Polym. J. 119 (2019) 272–280.

[42] Y. Chen, L.-R. Guo, W. Chen, X.-J. Yang, B. Jin, L.-M. Zheng, X.-H. Xia, 3-mercaptopropylphosphonic acid modified gold electrode for electrochemical detection of dopamine, Bioelectrochemistry. 75 (2009) 26–31.

[43] D.-S. Yang, D. Bhattacharjya, S. Inamdar, J. Park, J.-S. Yu, Phosphorus-Doped Ordered Mesoporous Carbons with Different Lengths as Efficient Metal-Free Electrocatalysts for

Oxygen Reduction Reaction in Alkaline Media, J. Am. Chem. Soc. 134 (2012) 16127–16130.

[44] F. Quesada-Plata, R. Ruiz-Rosas, E. Morallón, D. Cazorla-Amorós, Activated Carbons Prepared through H3PO4-Assisted Hydrothermal Carbonisation from Biomass Wastes: Porous Texture and Electrochemical Performance, Chempluschem. 81 (2016) 1349–1359.

[45] A.C. Ferrari, Raman spectroscopy of graphene and graphite: Disorder, electron–phonon coupling, doping and nonadiabatic effects, Solid State Commun. 143 (2007) 47–57.

[46] J.H. Lehman, M. Terrones, E. Mansfield, K.E. Hurst, V. Meunier, Evaluating the characteristics of multiwall carbon nanotubes, Carbon. 49 (2011) 2581–2602.

[47] N. Chakrapani, S. Curran, B. Wei, P.M. Ajayan, A. Carrillo, R.S. Kane, Spectral fingerprinting of structural defects in plasma-treated carbon nanotubes, J. Mater. Res. 18 (2003) 2515–2521.

[48] S. Leyva-García, K. Nueangnoraj, D. Lozano-Castelló, H. Nishihara, T. Kyotani, E. Morallón, D. Cazorla-Amorós, Characterization of a zeolite-templated carbon by electrochemical quartz crystal microbalance and in situ Raman spectroscopy, Carbon. 89 (2015) 63–73.

[49] G. Sócrates, G. Infrared and Raman Characteristic Group Frequencies. Tables and Charts, 3rd ed. Jhon Wiley & Sons, Ltd, Chichester, UK, 2004.

[50] M. A. Cotarelo, F. Huerta, C. Quijada, R. Mallavia, J. L. Vázquez. Synthesis and Characterization of Electroactive Films Deposited from Aniline Dimers. J. Electrochem. Soc, 2006, 153 (7) D114-D122.

[51] E. M. Geniès, J. F. Penneau, M. Lapkowski, A. Boyle. Electropolymerisation Reaction Mechanism of Para-Aminodiphenylamine. J. Electroanal. Chem. Interfacial Electrochem. 1989, 269 (1), 63–75.

[52] E. F. Antunes, A. O. Lobo, E. J. Corat, V. J. Trava-Airoldi, A. A. Martin, et. al.. Comparative Study of First- and Second-Order Raman Spectra of MWCNT at Visible and Infrared Laser Excitation. Carbon. 2006, 44 (11), 2202–2211.